GEOPHYSICAL MEASUREMENTS FOR SUBSURFACE MAPPING AND GROUNDWATER EXPLORATION AT THE CENTRAL PART OF THE SINAI PENINSULA, EGYPT

S.A. Sultan*

National Research Institute of Astronomy and Geophysics, 11722, Helwan,Cairo, Egypt
and University of Lisbon, Center of Geophysics-IDL, Campo
Grande Ed. C8, 1749-016 Lisboa, Portugal

Hatem M. Mekhemer

Water Resources Research Institute, National Water Research Center (NWRC) Egypt

F. A. M. Santos

University of Lisbon, Center of Geophysics-IDL, Lisboa, Portugal

and M. Abd Alla

National Research Institute of Astronomy and Geophysics

Cairo, Egypt

الخلاصة

إن تحديد الخزان الجوفي العميق هو الهدف الرئيسي من هذه الدراسة . تقع منطقة الدراسة في وسط سيناء، وهي من المناطق الجافة في مصر. وقد تم تطبيق العديد من الطرق الجيوفيزيقية مثل طريقة المقاومة النوعية ، والجاذبية الأرضية، والمغناطيسية الأرضية لاستكشاف المياه الجوفية. وقد تم قياس خمس عشرة جسة كهربية بمسافة بين الأقطاب تتراوح بين أب = 10 متر إلى أب = 6000 متر لإمكانية تحديد الخزان الجوفي العميق في منطقة الدراسة. وتم استخدام نماذج المقاومة النوعية أحادية البعد لتشييد القطاعات الجيوكهربية لتحديد الوحدات الاستجرافية التحت سطحية المكونة للخزان الجوفي. وقد أظهرت القطاعات الجيوكهربية أن الجزء العلوي من القطاع التحت سطحي يتكون من أربع وحدات صخرية. ويمثل الخزان الجوفي العميق الوحدة الرابعة التي تتكون من الحجر الرملي النوبي (رواسب عصر الطباشيري السفلي)، وعمق السطح العلوي للحجر الرملي النوبي يتراوح بين 300 إلى 1000 متر. والمقاومة النوعية للخزان الجوفي تتراوح بين 60 إلى 400 أوم. متر وتحتوي على مياه جيدة النوعية.

وقد تمّت قياسات الجاذبية الأرضية والمغناطيسية (المركبة الكلية للمجال المغناطيسي) من خلال مائة وخمسين محطة. والتفسير المشترك لبيانات المغناطيسية والجاذبية الأرضية سمح بتحديد عمق صخور القاعدة الجرانيتية وسطح الكنوراد. وقد أبانت نتائج النماذج المستخلصة أن عمق صخور القاعدة يتراوح بين 1500 إلى 3150 متر وعمق سطح الكنوراد يتراوح بين 7130 إلى 8730 متر. والتراكيب الجيولوجية التي تقطع منطقة الدراسة معظمها من النوع العادي ، وتأخذ اتجاهات شمال غرب-جنوب شرق وشمال – جنوب وشمال شرق- جنوب غرب. هذه التراكيب الجيولوجية مرتبطة بالحركات الأرضية الرأسية التي يمكن أن تكون قد تحكمت في ترسيب الوحدات الصخرية المختلفة.

---

* Address for correspondence
Sultan Awad Sultan Araffa
National Research Institute of Astronomy and Geophysics, 11722, Helwan, Cairo, Egypt.
E-mail : sultan_awad@yahoo.com
Tel; +20225560645
Mobile: +20122588505
Fax: +20225548020

S.A. Sultan, Hatem M. Mekhemer, F. A. M. Santos, and M. Abd Alla

ABSTRACT

Characterization of a deep aquifer is the main target of the research work presented here. The study area is located in the central part of Sinai, an extremely arid region in Egypt. Different geophysical methods, including resistivity, gravity, and magnetic, were applied in the study area for groundwater exploration.

Fifteen vertical electrical soundings were measured with current electrode spacing ranging from AB = 10 m to AB= 6000 m, in order to detect the deep aquifer in the study area. The resistivity 1D models were used to construct a geoelectrical cross-section to define the subsurface stratigraphy units, including the water-bearing aquifer. The geoelectrical cross-sections showed that the upper part of the subsurface consists of four geoelectric units. The deep aquifer is lodged by the last unit constituted of Nubian sandstone (Lower Cretaceous deposits). The depth of the top of the Nubian sandstone ranges between 300 and 1000 m. The resistivity of the aquifer varies between 60 and 400 ohm-m, indicating the existence of good quality water.

Gravity and ground magnetic (total magnetic field) measurements were made at one hundred and fifty stations. The combined interpretation of the magnetic and gravity data allowed the determination of the depth of the surface of the granitic basement and the depth of the Conrad surface. The results of the modeling indicate that the basement lies between 1500 and 3150 m depth and that the Conrad surface (interface between the granitic and basaltic layer) is ranging from 7130 to 8780 m. Structural elements (mostly normal faults) NW-SE, N–S and NE–SW oriented, have been detected. These structures are associated with vertical movements that might have controlled the sedimentation of the uppermost geological formations.

Key words: gravity, magnetic, resistivity, groundwater

GEOPHYSICAL MEASUREMENTS FOR SUBSURFACE MAPPING AND GROUNDWATER EXPLORATION AT THE CENTRAL PART OF THE SINAI PENINSULA, EGYPT

1. INTRODUCTION

Integrated geophysical tools, especially resistivity, electromagnetic and, more recently, nuclear magnetic resonance methods, are commonly used in groundwater exploration, mainly due to the close relationship between electrical conductivity and some hydrological parameters [1]. The resistivity method is used for detecting groundwater presence and differentiating subsurface layers. The gravity method is also used in groundwater exploration and in the detection of structural trends controlling the regional geometry of the groundwater aquifers [2]. The magnetic method is an important tool to detect the upper surface of the basement and, indirectly, the thickness of the sedimentary cover. Several authors have been using integrated geophysical interpretation in groundwater exploration at different areas in Sinai. Hassanen *et al.* [3] used resistivity, gravity, and magnetic methods for groundwater exploration at Nukhil area in central Sinai. Sultan and Sorady [4] used geoelectrical and gravity to study the structural elements and groundwater exploration in a region located northwest of Sinai. Recently, Monteiro Santos *et al.* [5] have used joint inverse of resistivity and gravity data for groundwater exploration in the northwestern part of Sinai.

This paper presents a geophysical study to evaluate the groundwater potential and to map the geologic subsurface structures

2. GEOLOGICAL SKETCH

The study area lies around Wadi Al Ghubba in the north Egma plateau (central part of Sinai) and is located between latitudes 29° 28′ and 30° 03′ and between longitudes 33° 07′ and 33° 50′ (Figure 1). The area is inhabited by Bedouins, suffering from a scarcity of water necessary for domestic use. The lowlands and wadis represent the greater part of the study area. The main surface geology is described in the geological map of Sinai at a scale of 1:500 000, performed by UNSECO Cairo Office [6] and is shown in Figure 2. The area is mostly covered by Pleistocene deposits composed of alluvium deposits and Paleocene deposits including Esena Shale Formation, which is composed of marly shale. Different geologic units from the Lower Eocene to Upper Cretaceous cover the eastern part of the area. Egma Formation of chalky limestone represents the Lower Eocene deposits. The Upper Cretaceous is represented by Sudr Formation, which is composed of chalk of Maastrichtian age, Duwai Formation composed of alternated carbonate and clastic of Campanian age, Matullah Formation, which is composed of limestone of Conician–Santonian age, and Wata Formation, composed of dolomitic limestone of Conician–Turonian deposits.

3. GEOPHYSICAL DATA ACQUISITION AND INTERPRETATION

3.1. Geoelectrical Data

The geoelectrical data used in this study consist of fifteen vertical electrical soundings (VES), using the Schlumberger configuration with AB/2 spacing ranging from 5m to 3000 m. The main objective is to detect the Nubian sandstone aquifer in the study area (Figure 3). The data were acquired using the CH-8708A transmitter and the EPR0121A recorder along with the inverted non-linear approach. One of the soundings, the VES 13, was carried out coincidently with the borehole JICA1. The VES 10 was measured near the borehole JICA3. The geological data obtained from JICA1 were used in the calibration of the geoelectrical models obtained from the apparent resistivity curves. Table 1 summarizes the geological information obtained from the JICA1 borehole. Figure 4 shows the correlation between geoelectrical parameters and the geology obtained from VES 13. The electrical measurements were carried out along the wadis (valleys) trends in the N–S and NE–SW directions.

There are several methods for VES data interpretation: graphical (manual) and analytical methods. The authors used a manual (graphical) interpretation, which depends upon matching the plotted field curves with the standard curves and the generalized Cagniard graphs [7].

The obtained results of the manual interpretation were used as initial models for the analytical methods. The quantitative interpretation was made using the IPI2WIN program. The IPI2WIN program was designed by a scientific group in Moscow State University, Russia in 2000. The quantitative interpretation has been applied to determine the thicknesses and true resistivities of the stratigraphic units below each VES station.
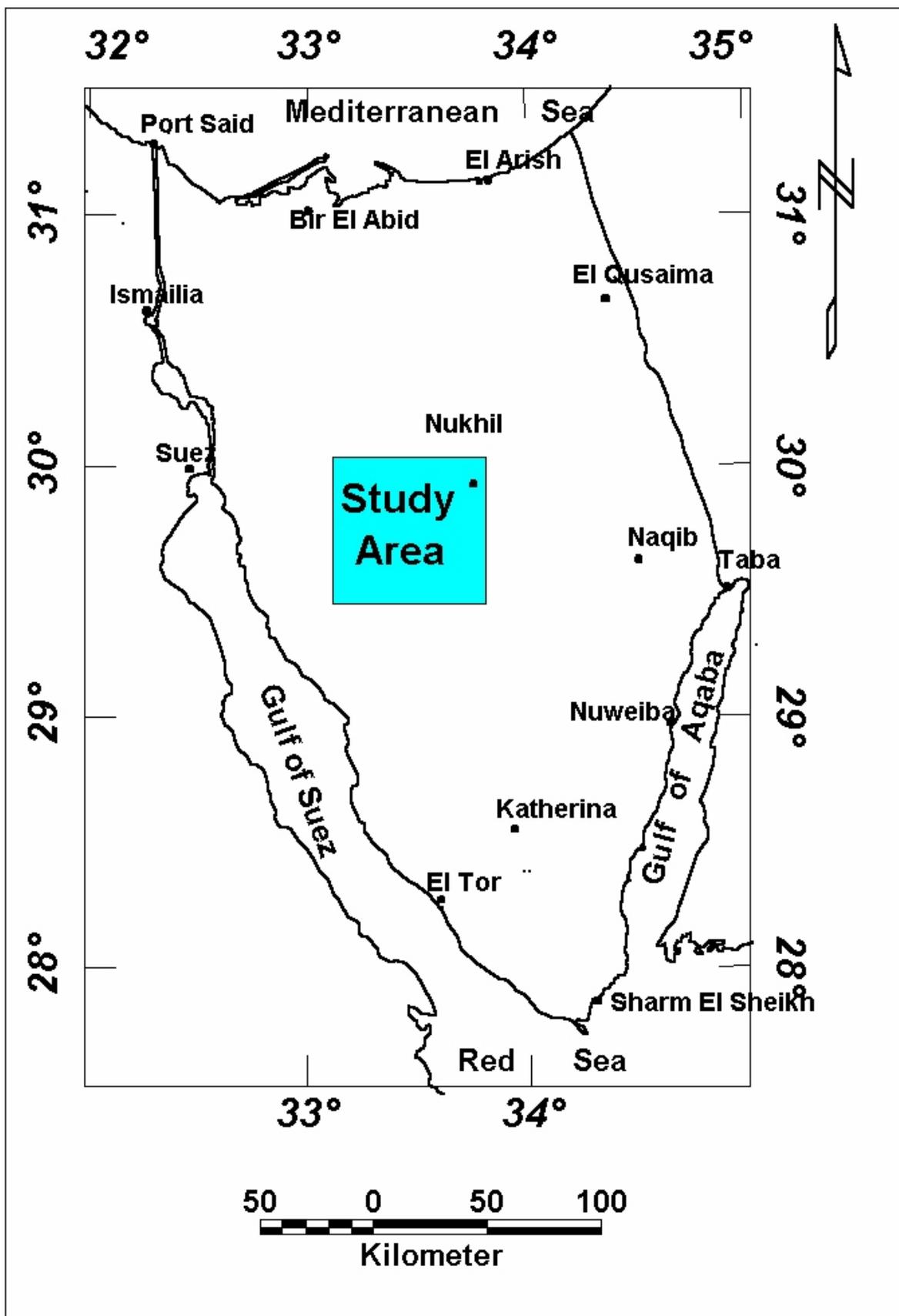
S.A. Sultan, Hatem M. Mekhemer, F. A. M. Santos, and M. Abd Alla
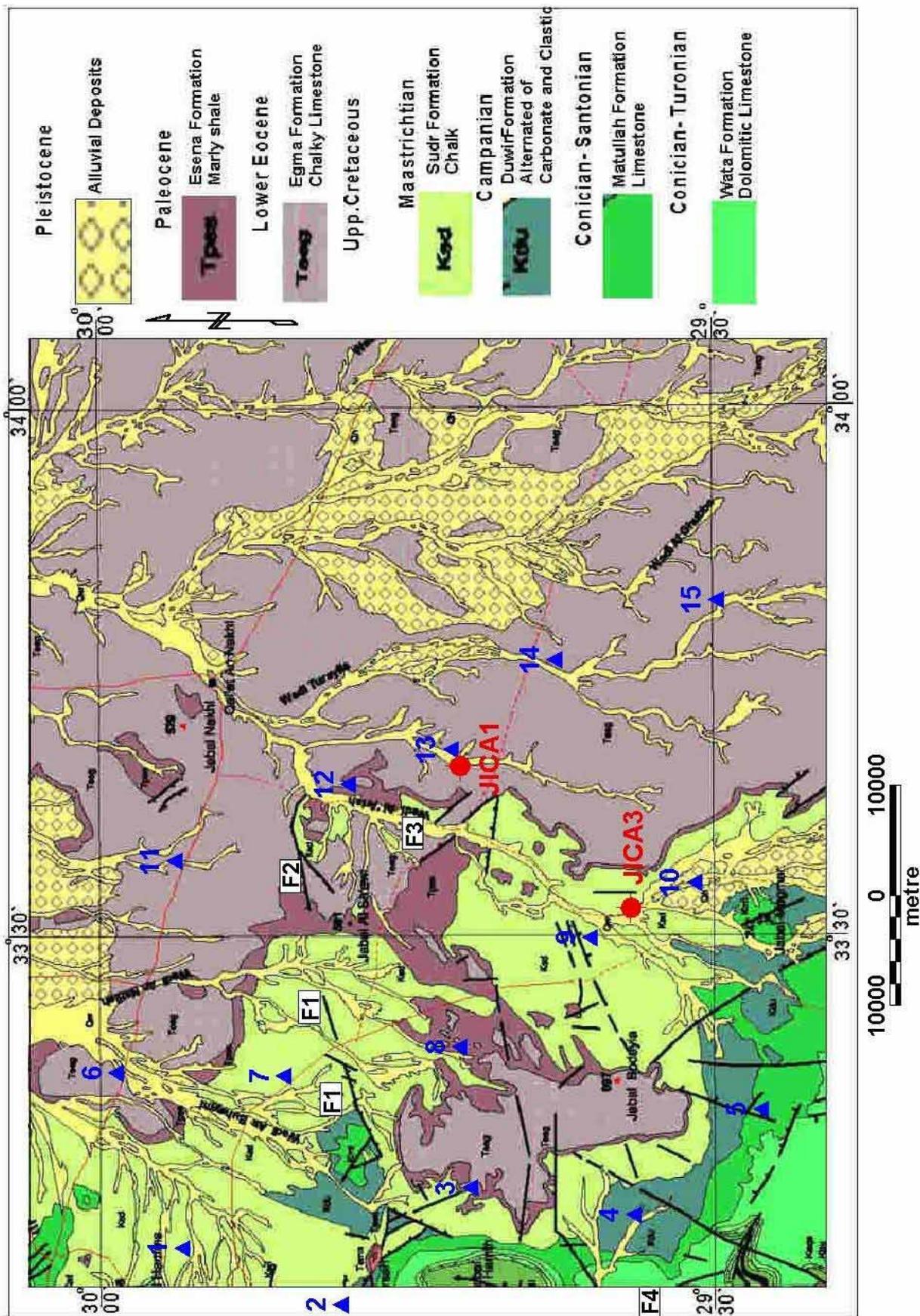
Figure 1. Location map of the study area

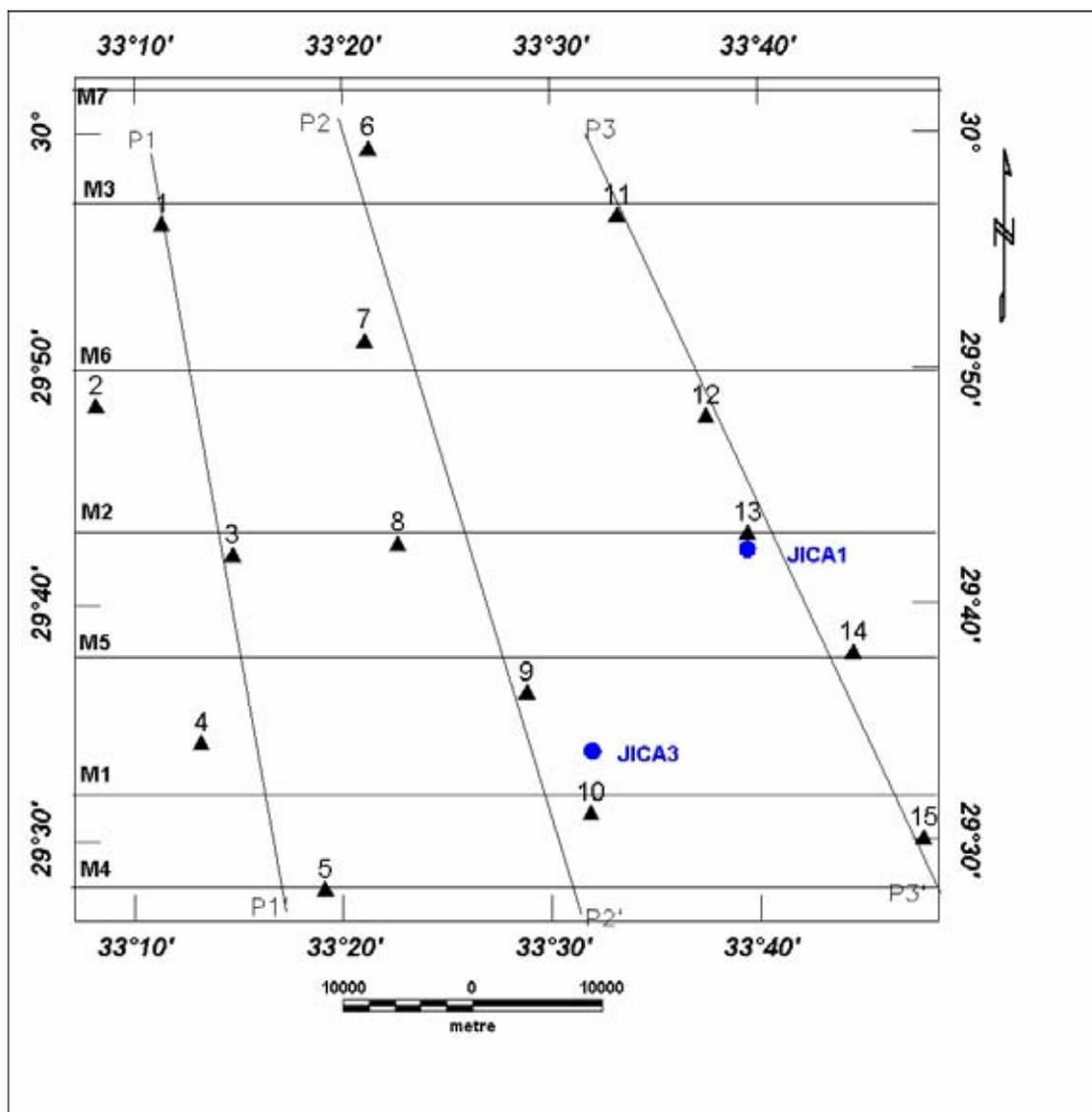Figure 2. Geological Map of the Study Area (after [6])

Figure 3. Location map of the boreholes, VES, and gravity–magnetic modeled profiles

Table 1. Geological Description of the Borehole JICA 1

| Depth (m) | | Age | Description |
From	To		
0	50	Paleocene	Wadi Deposits
50	180	Maastrichtian	Limestone intercalated with clay
180	270	Campanian	Claystone
270	385	Santonian-Coniacian	Limestone intercalated with clay
385	450	Turonian	Limestone
450	520		Chalky Limestone
520	585	Cenomanian	Limestone intercalated with clay
585	640		Limestone
640	670		Limestone intercalated with clay
670	700		Limestone
700	770		Limestone intercalated with clay
770	810		Limestone
810	865		Limestone intercalated with clay
865	1115	Lower Cretaceous	Alternation of shale and Sandstone
1115	1260	Jurassic	Sand and Shale
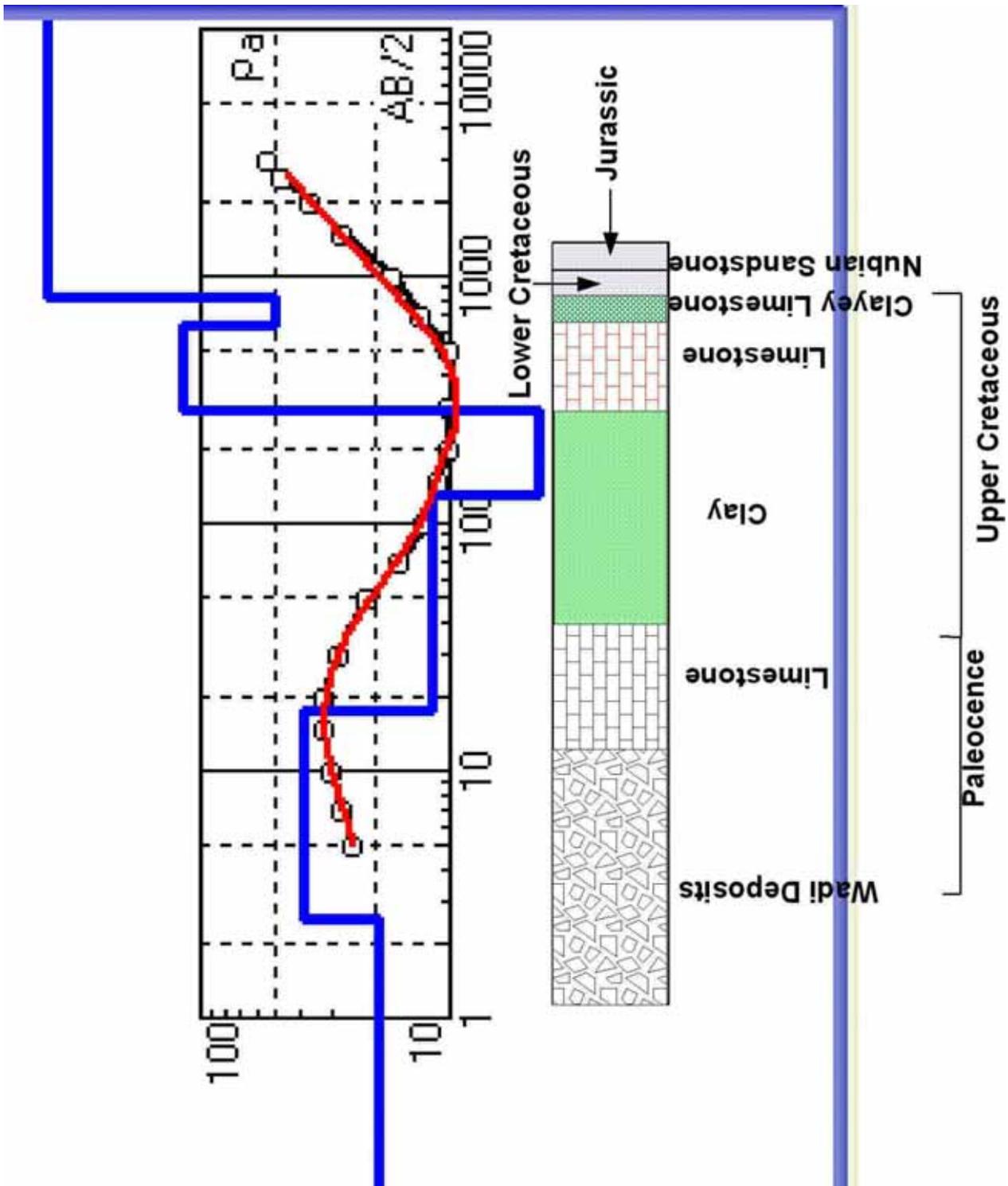
Figure 4. Resistivity model obtained from the inversion of the VES 13 and its correlation with the geological-log obtained from the borehole JICA1 (see also Table 1)

3.2. Gravity Data

The CG-3 Autograv (automated Gravity meter) of Scintrex was used in the gravity survey. This type of gravity meter is a microprocessor-based automated meter with numerous revolutionary features. It is based on a fused-quartz elastic system. The CG-3 combines a measurement range of over 7000 mgals without resetting and a reading resolution of 0.01 mGals. These two features enable the gravity meter to be used for detailed local investigation and comprehensive regional survey as well as for large scale geodetic studies. Based upon geographic location and time zone information entered by the operator, the Autograv automatically calculates, and applies, a real time tidal correction to each reading. Also, a real time software correction reduces the drift of the instrument to less than 0.02 mgals per day. Finally, the header information, observed values, station numbers, line number, and time for each observation are all recorded for each measurement in the standard and internal 48K ram solid-state memory. One-hundred and fifty gravity stations were utilized covering the study area, with spacing between the stations ranging from 2–5 km, according to the accessibly of the sites, which was strongly controlled by the topography of the study area. Different corrections (drift, tide, latitude, free-air, and Bouguer) were performed using the specialized Geosoft program [8]. Terrain correction was also carried out using the Bible chart to estimate the elevation points of different zones.

The corrected gravity values were used to construct a Bouguer anomaly map by using Oasis Montaj software with a contour interval of 1 mGal (Figure 5*a*). The map shows a gravity gradient with a NW–SE direction, correlating with the transition from Paleocene and Lower Eocene to Upper Cretaceous formations. High-pass and low pass filter techniques were used to decompose the Bouguer anomaly into the components related to shallow depths (residual anomalies) and those from deeper sources (regional anomalies). The separation was carried out applying filter techniques and a cut-wave number of 0.0002 km^{-1}. The regional Bouguer anomaly map (Figure 5*b*) indicates that the deep-seated sources are deeper at the northeastern part and become shallower towards southwest. The residual Bouguer anomaly map (Figure 6*a*) indicates different trends of the structural elements such as NE–SW and NW–SE trends (Figure 6*b*).

3.3. Magnetic Data

Total intensity magnetic field measurements were carried out at the gravity stations with two Envimag Proton magnetometers made by Scintrex Company of Canada with one 1 nT sensitivity. One magnetometer was used for base station recordings, to apply the diurnal variation correction, and the other one was used for field measurements. The obtained values were corrected for the normal gradient of the earth's magnetic field (IGRF); the corrected magnetic values were contoured using Oasis Montaj software. The final result is a total intensity magnetic map as shown in Figure 7. The magnetic fields created by geological bodies are distorted by the inclination and declination of the earth's field making it difficult to estimate correctly the shapes and locations of these magnetized bodies. In order to overcome this distortion in the appearance of an anomaly, which depends on the magnetic latitude of the survey area and on the dip angle of the magnetization vector in the body, a mathematical procedure is adopted on a grid of values of the contour map of the total magnetic intensity. Therefore, the interpretation of the magnetic data starts with the conversion of the total intensity map into a more interpretable map: then this is reduced to a magnetic pole map. This mathematical procedure was first described by Baranov [9], Baranov and Naudy [10], Battacharyya [11, 12], and Baranov [13].

The total intensity magnetic map after being reduced to the pole (Figure 8*a*) indicates that the northern and southwest of the study area are occupied by high magnetic structures while the eastern part is represented by low magnetic structures. The total intensity magnetic map reduced to the pole was used for estimate the depth and directions of the magnetic bodies through applying GRIDEPTH program which is part of the Geosoft programs package [8]. The method is based on the Euler's homogeneity equation which relates the magnetic field and its gradient components to the location of the source, with the degree of homogeneity *N*, which may be interpreted as a structural index [14]. The structural index is a measure of the rate of change of a field with distance. For example, the magnetic field of a narrow 2-D dyke has a structural index of $N = 1$, while a vertical pipe (or cylinder) has $N = 2$. The magnetic field originated by a step (1) and contact has $N = 0$. The depth of the magnetic sources in the survey area was estimated using different structural index of 0, 1, 2, and 3. Only solutions for $N = 0$ produced real results which are plotted to represent the depths and directions of the magnetic sources as shown in Figure 8*b*. The depths of the magnetic sources ranged between less than 1000 m and 7000 m and have trends N–S, NE–SW, and NW–SE.

4. RESULTS AND DISCUSSION

The final 1-D inversion results of VES interpretation have been used for the construction of three geoelectrical cross sections using Oasis Montaj (Geosoft) software. The three geoelectric cross-sections were constructed along three profiles oriented approximately N–S. The cross-sections are shown in Figures 9*a*, *b*, and *c* combined with gravity profile with a geological interpretation of the layers. The models in the cross-sections indicate that the shallow subsurface lithological sequence, in the study area, is represented by four geoelectric units with relative

resistivities in accordance with the following pattern: $\rho_1 < \rho_2 > \rho_3 < \rho_4$. The upper units, corresponding to clay, are characterized by low resistivity values ranging from 5 to 70 ohm-m with total thickness varying from 80 to 276 m. The second geoelectric unit, which is associated to limestone, shows relatively high resistivity values ranging from 6 to 145 ohm-m and thickness ranging from 26 to 404 m. The third geoelectric unit is characterized by relatively low resistivity values (2–60 ohm-m). Lithologically, this unit consists of limestone intercalated with clay and contains saline and brackish water. The fourth unit is characterized by relatively high resistivity values ranging from 64 to 412 and corresponds to sand and sandstone. According to the borehole results this unit contains the main (fresh water) groundwater aquifer in the area. The bulk resistivity values of this layer suggest that the water is, in general, of good quality.

Through the interpretation of gravity and resistivity data, it is possible to identify the location of three faults affecting the sedimentary cover. The fault F1 crosses the western profile between VES 2 and VES 3, the F3 crosses the middle profile between VES 7 and VES 8. The eastern profile is crossed by a fault F2 between VES 12 and VES 14 (Figure 2 and Figure 5*a*). The combined interpretation of the residual Bouguer map and the geoelectrical models suggest that the basement might be compartmented by the ENE–WSW fault (F1) and the NW–SE fault (Figure 2) with the uplift of the southwestern block. The solutions of Euler deconvolution indicates that deeper faults extended in the basement and shallower faults extended in the sedimentary (Figure 8*b*).

The principal application of the magnetic and gravity data is to determine the depth of the anomalous sources of the observed anomalies. The quantitative interpretation of the magnetic and gravity data map was carried out through trial-and-error modeling, assuming the 2D approach. In this work seven profiles trending W–E were modeled (Figure 10). Densities of 2.39 gm/cm^3 for sedimentary cover, 2.7 gm/cm^3 for the basement complex, and 3.2 gm/cm^3 for the basaltic layer were assumed in accordance with the published values [15]. The magnetic susceptibility of the basement was assumed to be a constant with a value of 0.00535 cgs unit (0.0672 SI unit). These parameters were used in the modeling of the seven profiles. The results of the combined modeling of gravity and magnetic data are shown in Figure 10. It is evident that the gravity and magnetic profiles correlate well with each other in response to the depth of the granitic basement surface, except for model (*c*). This may be attributed to a shallow fractured basement which decreasing the density with no effect on the magnetic response. The models in Figure 10 show the variations in the thickness of the sedimentary deposits and of the topography of the top of the granitic basement. These results were used to draw the map of the depth of the basement surface and the map of the depth of the Conrad surface, which separate the granite from the deep basaltic formations. The basement surface map (Figure 11), together with a sketch of the main geologic patterns, reveal that the basement is deeper at the eastern part of the area, reaching a depth of 3150 m, and becomes shallower at the northwestern part (mostly coincident with the Egma and Sudr Formations) with a depth of 1500 m. This result agrees very well with the interpretation of the resistivity cross-sections, and indicates that the sedimentary cover was controlled by tectonics movements occurred in the basement. The map of Figure 12 indicates that the Conrad surface is deeper at the northwestern part of the area, with a depth of 8785 m and is shallower at the southern part of the area reaching a depth of 7135 m.

CONCLUSIONS

The results obtained from the integrated interpretation of the resistivity, gravity and magnetic data agree with the boreholes data and the geology of the study area. The results revealed the existence of four major resistivity units with resistivity values ranging from 2 and 412 ohm-m and thickness between 1.4 and 462 m. The first unit consists of clay and has low resistivity values. The second unit shows high resistivity values representing limestone. The third one consists of limestone intercalated with shale and has low resistivity values. The fourth unit is characterized by relative high resistivity values and correlates with sand, and sandy clay and sandstone, which represents the main aquifer in the area. The top surface of the deep aquifer is probably at a depth ranging from 300 to 1000 m, being shallow in the southwestern part of the survey area. The interpretation of the gravity data shows that the main structural elements are well correlated with the Gulf of Aquba (NW–SE), the Gulf of Suez (NW–SE) and with the Nile Valley (N–S) trends. From the gravity and magnetic profiles, the thickness of the granitic basement is estimated to be within a range of 1500 m and 3150 m, and the depth to the Conrad surface ranging from 7135 m to 8783 m. The results also indicate that the evolution of the sedimentary cover might be controlled by the structural tectonics of the basement.
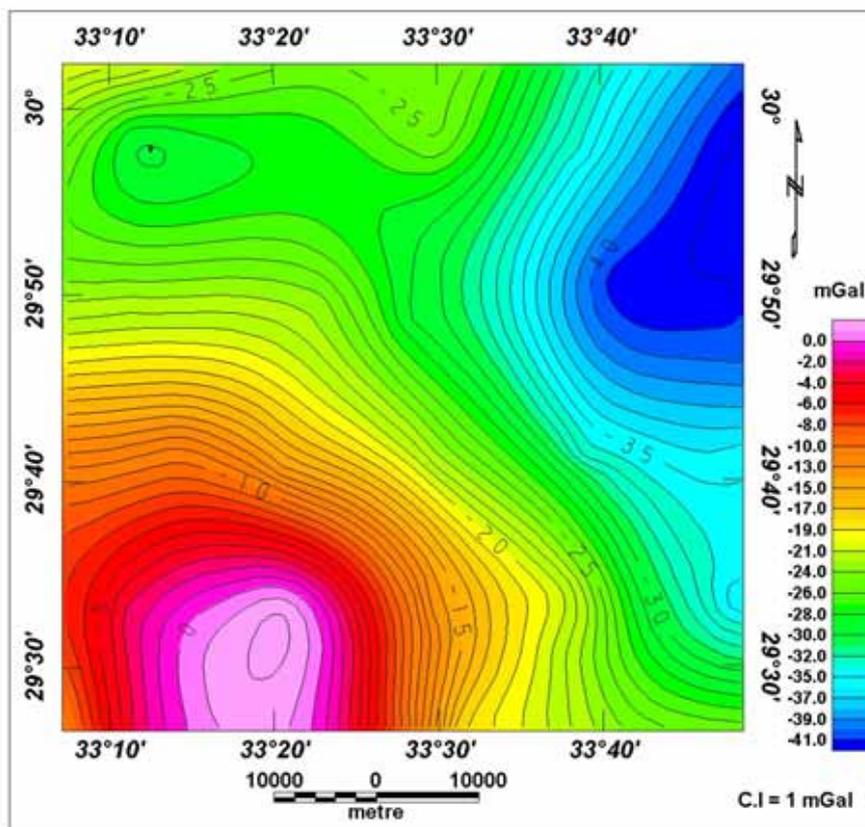
ACKNOWLEDGEMENTS

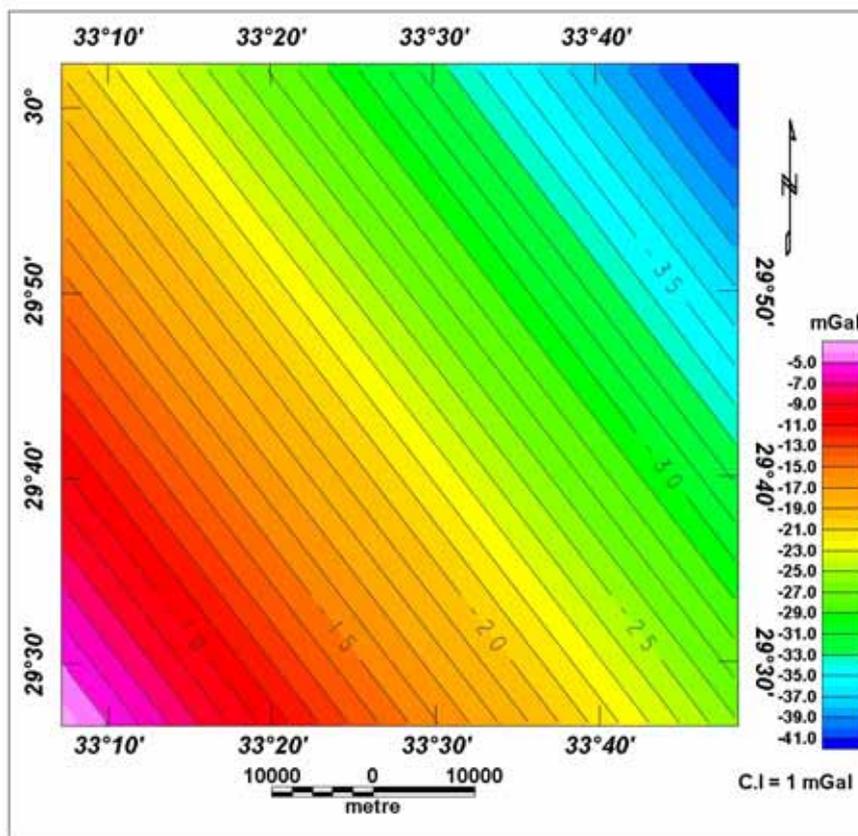*Figure 5a. Bouguer anomaly map*
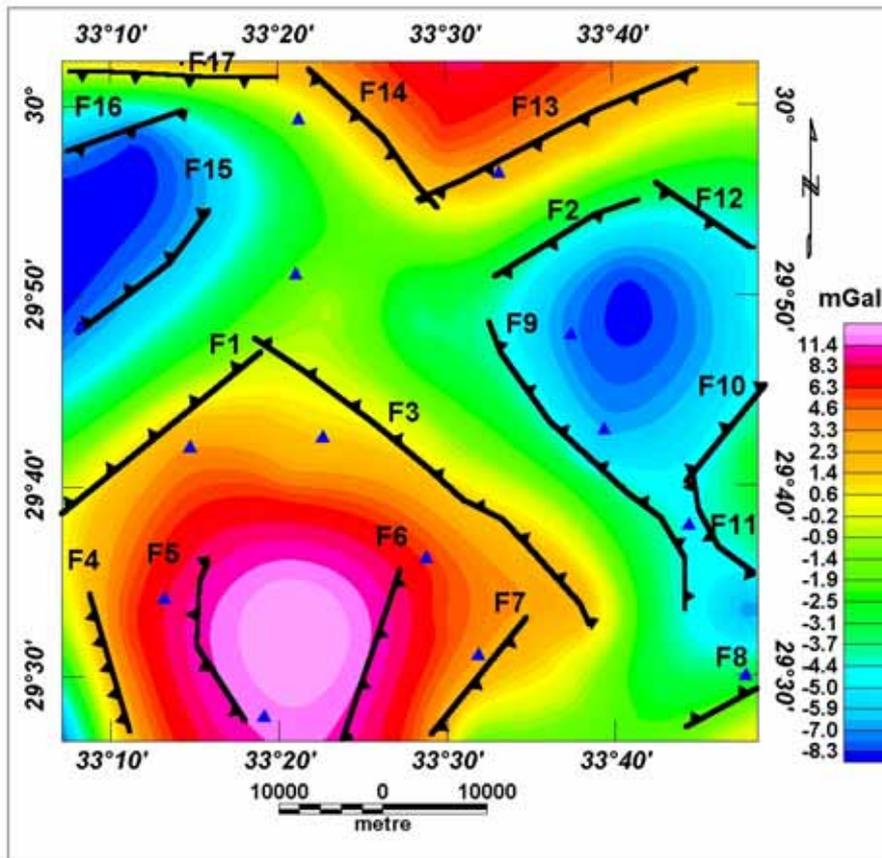

Figure 5b. Regional gravity map

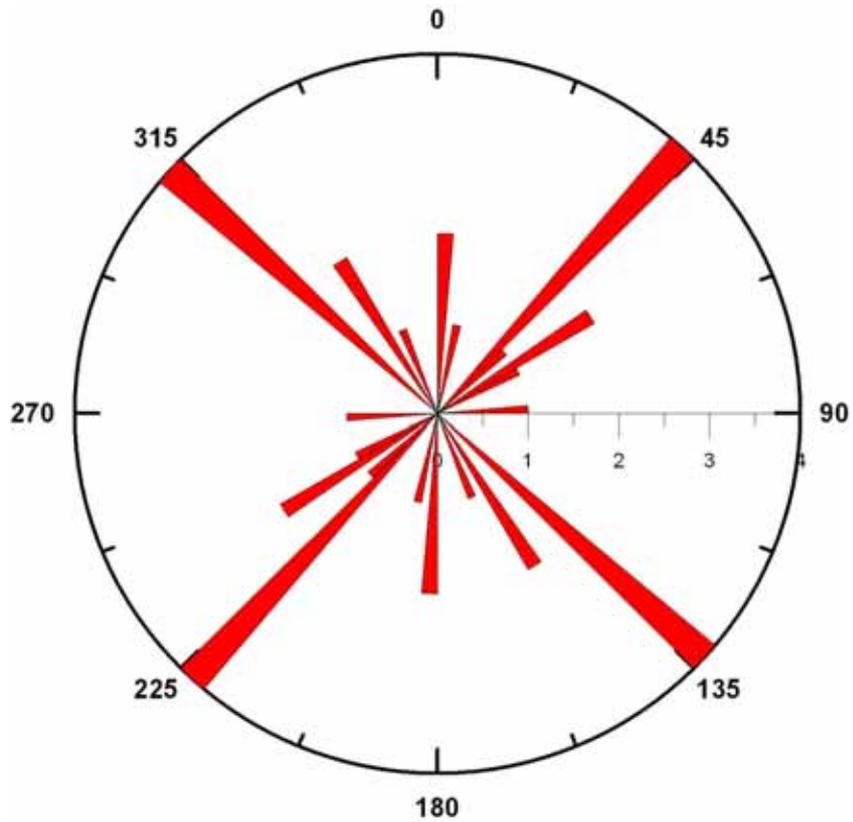*Figure 6a. Residual Bouguer anomaly map obtained by filtering*

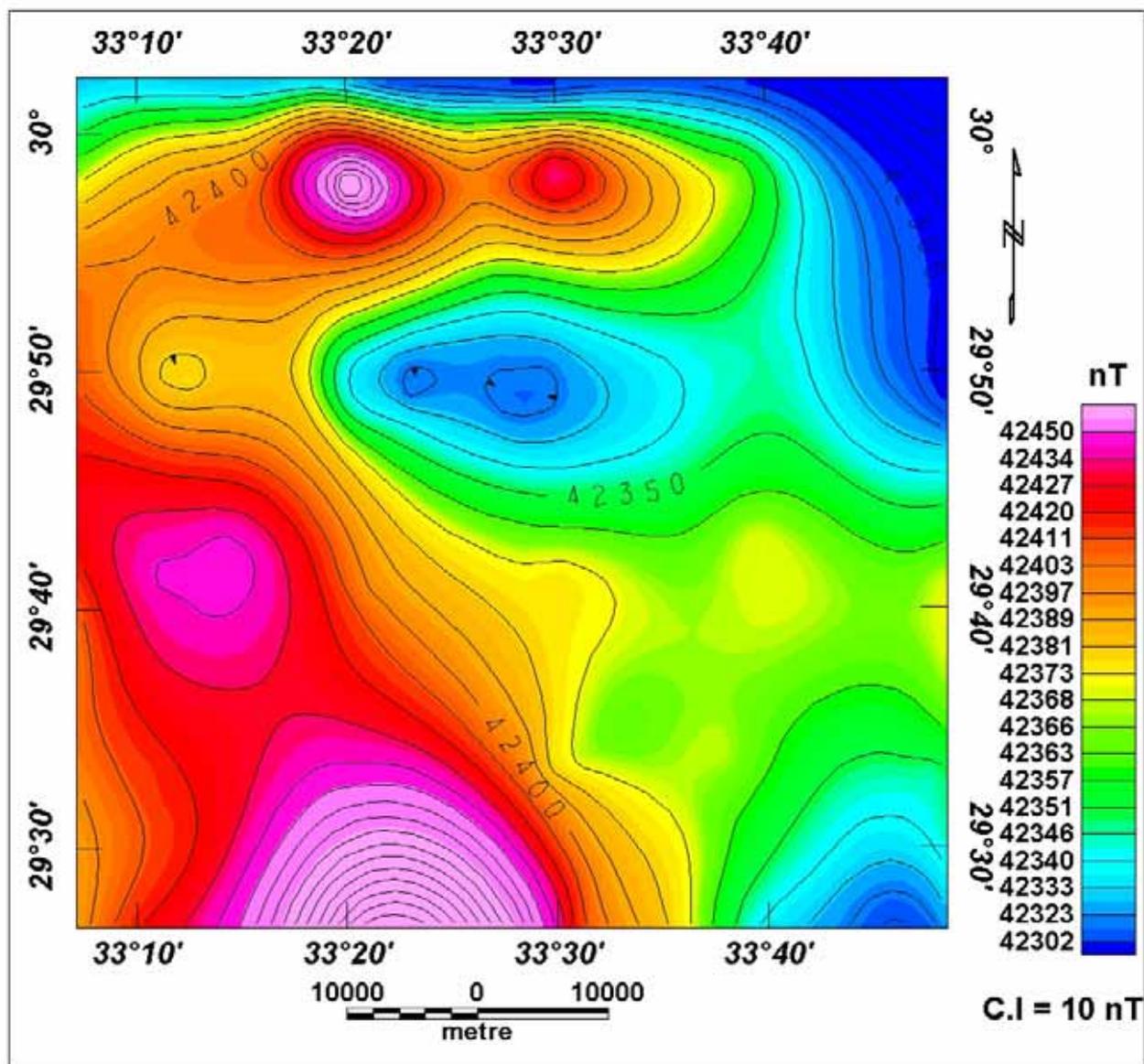*Figure 6b. Rose Diagram for the fault elements detecting from residual Bouguer anomaly map*

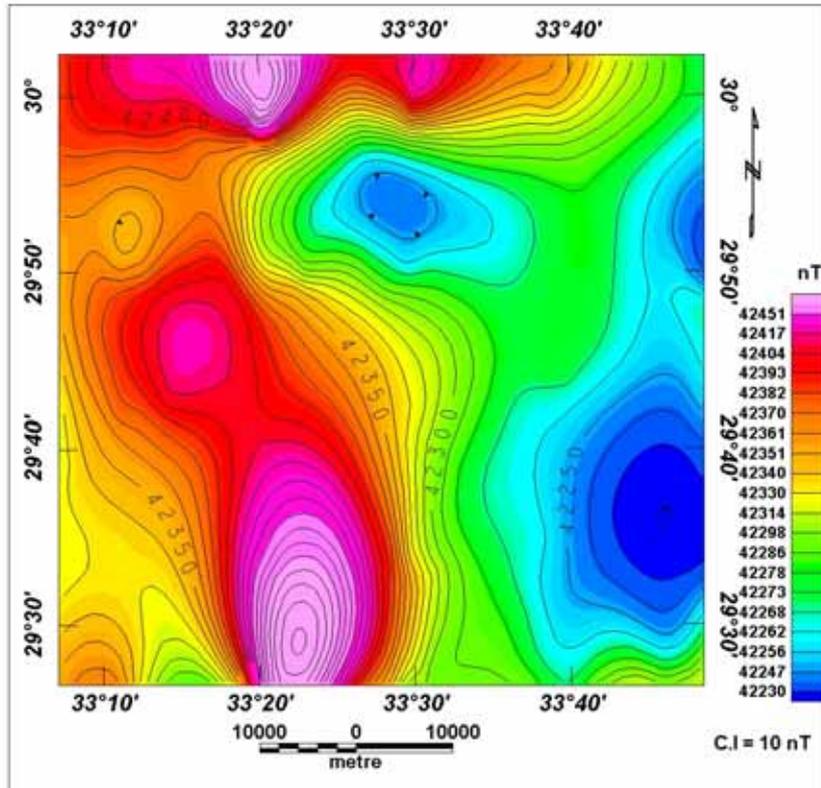*Figure 7. Total intensity magnetic map*

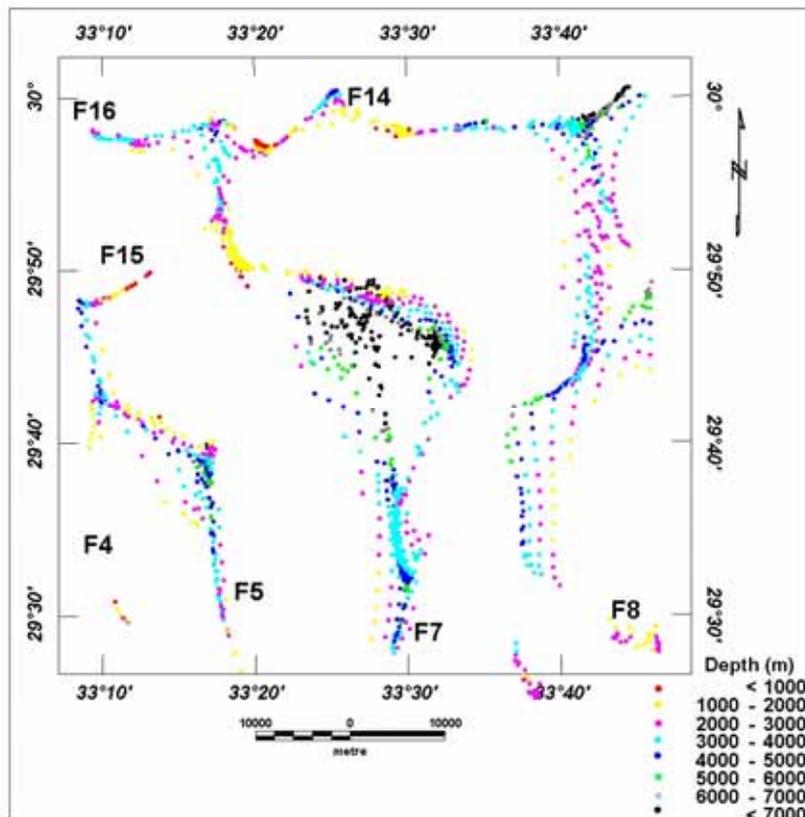*Figure 8a. Total intensity magnetic field reduced to the Pole*

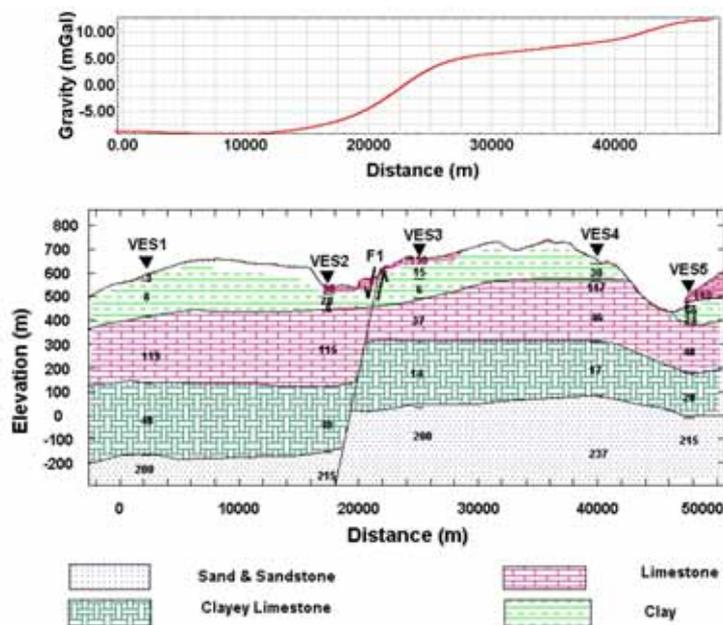*Figure 8b. Solution of Euler deconvolution using structural index (N) 1*

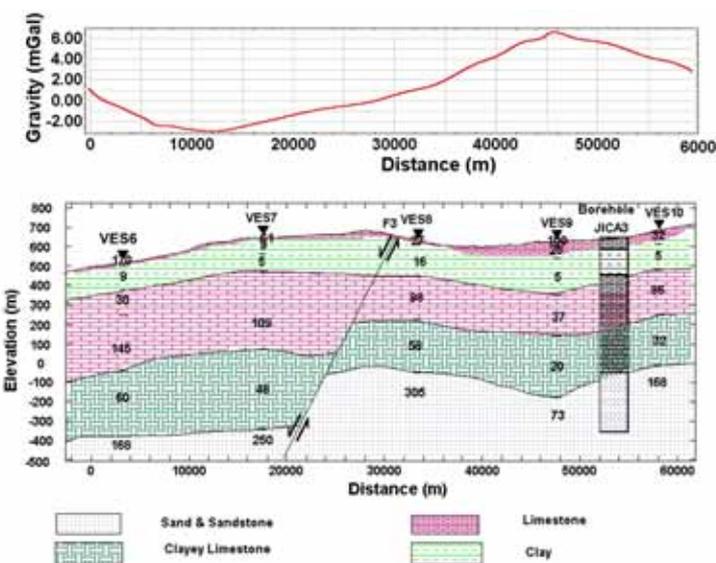*Figure 9a. Geoelectric cross-section along VES no.1, 2, 3, 4, and 5*

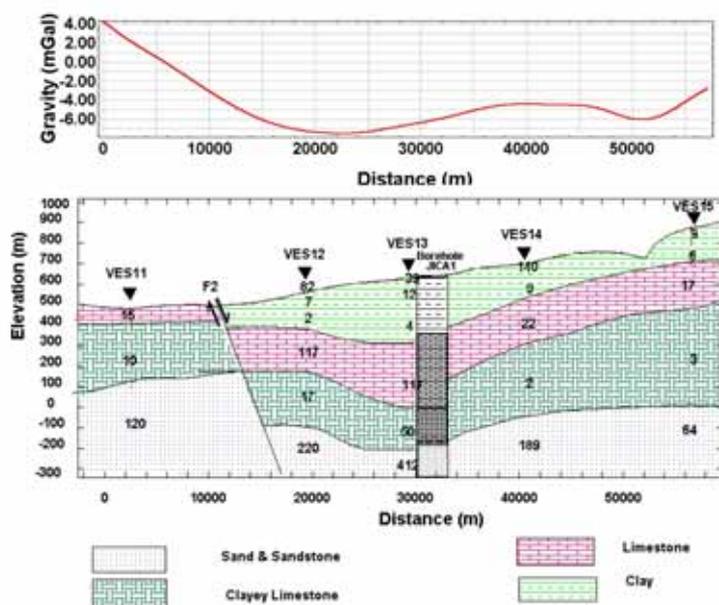*Figure 9b. Geoelectric cross-section along VES no.6, 7, 8, 9, and 10*

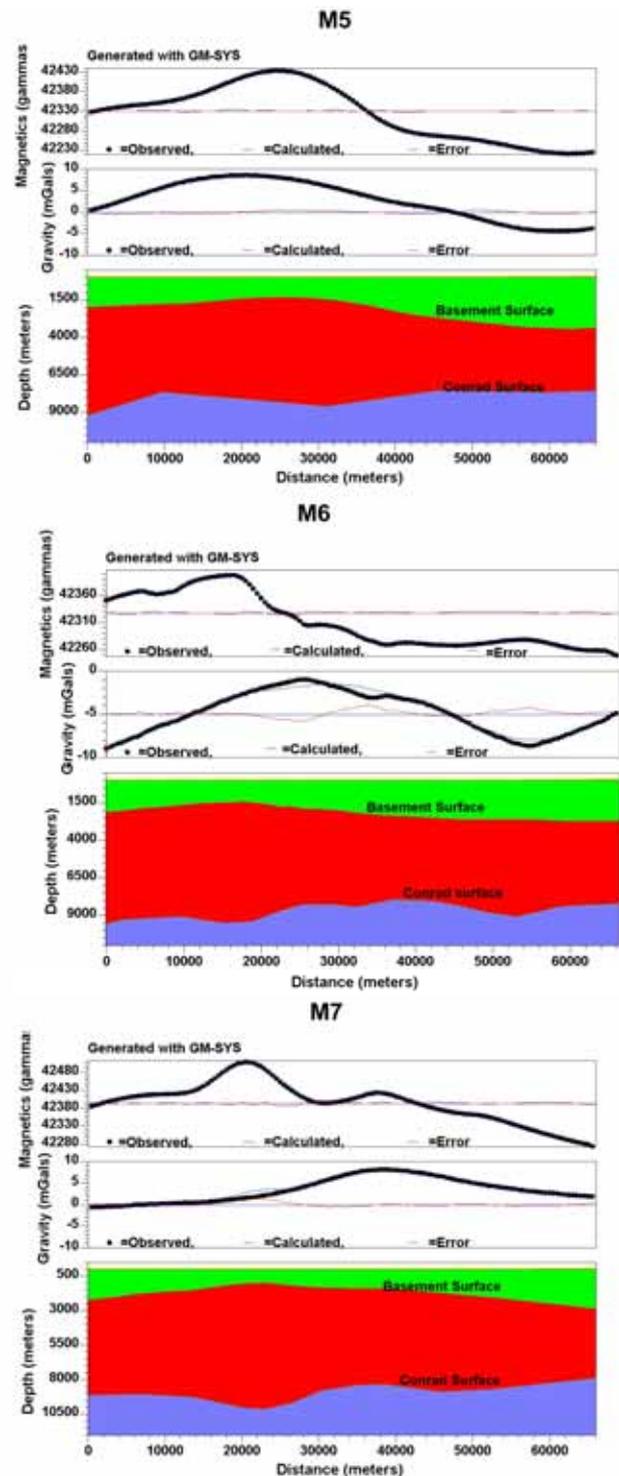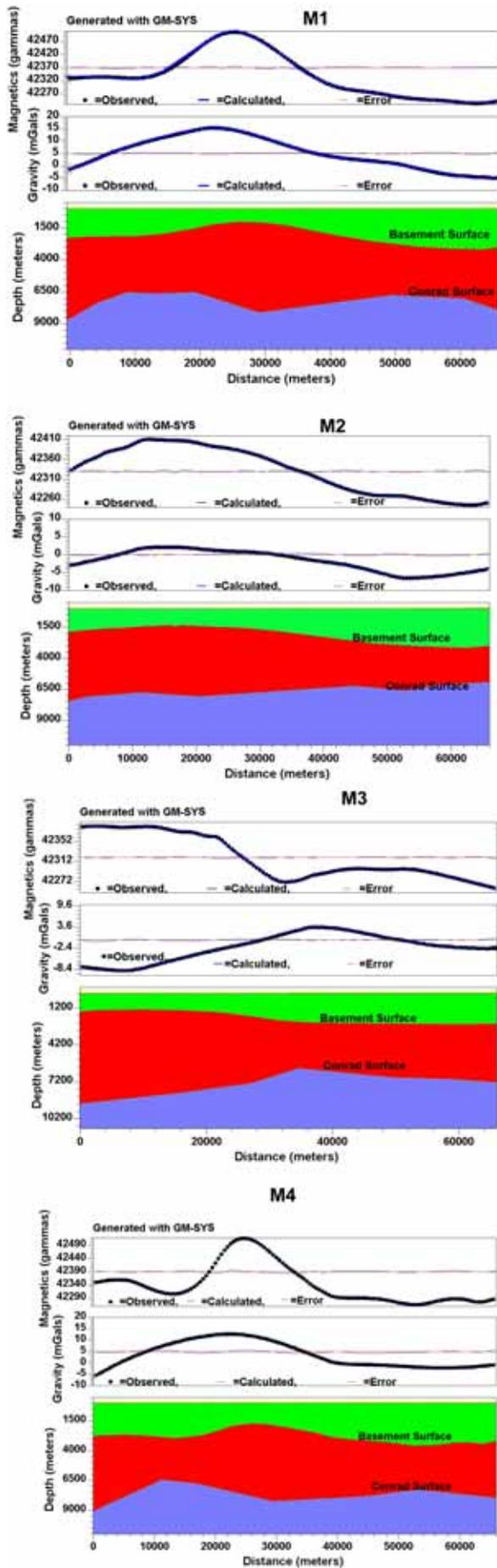*Figure 9c. Geoelectric cross-section along VES no.11, 12, 33, 14, and 15*

Figure 10(a) (Left) Gravity and magnetic models along profiles M1 to M4

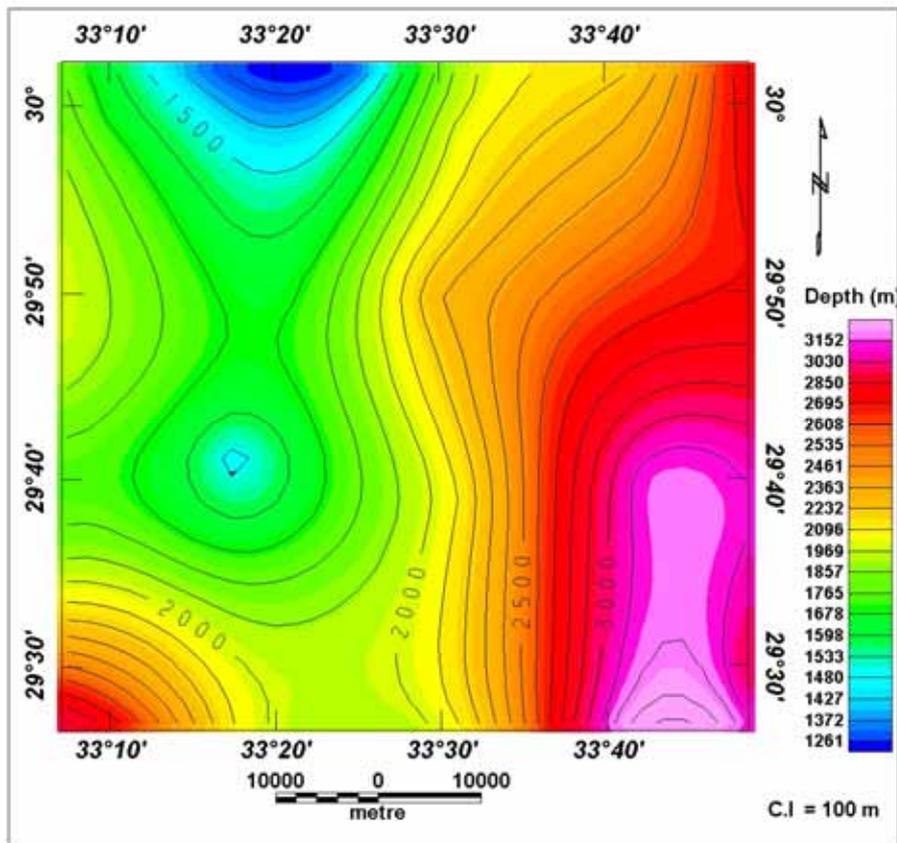*Figure 10(b) (Right) Gravity and magnetic models along profiles M5 to M7*

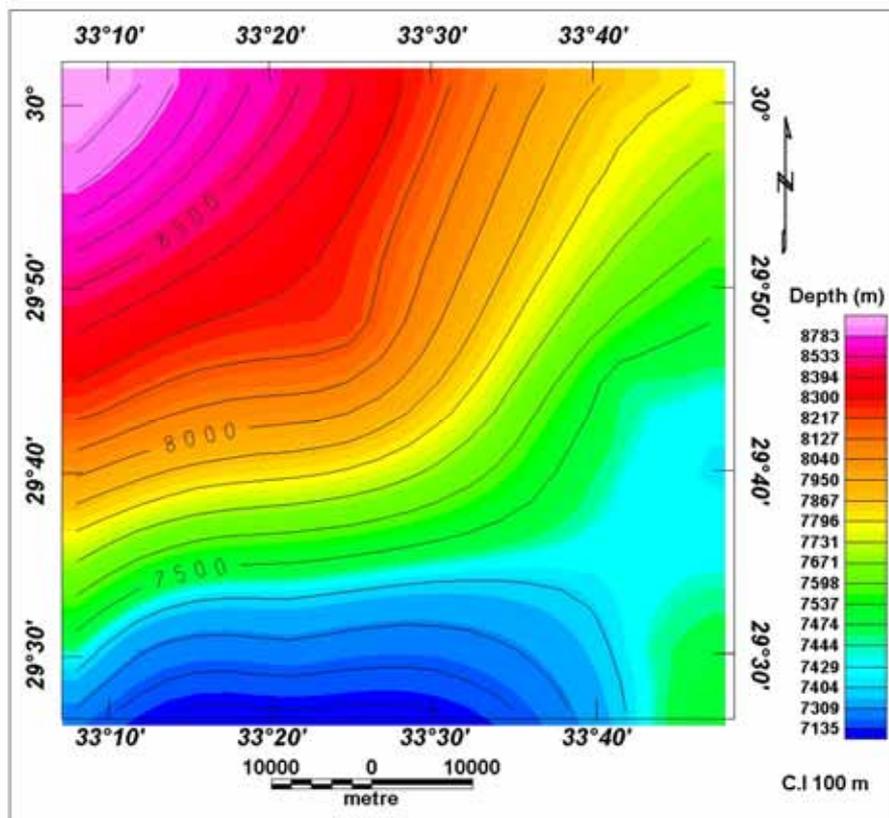*Figure 11. Depth to the basement surface. Scale of colors in m*

Figure 12. Depth to the Conrad surface. Scale of colors in m

REFERENCES

[1] M. Goldman and F.M. Neubauer, "Groundwater Exploration Using Integrated Geophysical Techniques", *Surveys in Geophysics*, **15**(**3**)(2004) pp. 331–361.

[2] B.V.S. Murty and V.K. Raghavan, "The Gravity Method in Groundwater Exploration in Crystalline Rocks: a Study in the Peninsular Granitic Region of Hyderabad, India", *Hydrogeology Journal*, **10**(2002), pp. 307–321. DOI.10.1007/s10040-001-0184-2.

[3] A. Gh. Hassanen, S. A. Sultan, and B. S. Mohamed, "Integrated Geophysical Interpretation for Groundwater Exploration at Nukhl Area, Central Sinai", *Bul. of National Res. Inst. Astronomy & Geophysics, Ser. B*, 2001, pp. 283–298.

[4] S. A. Sultan, and A. L. El Sorady, "Geoelectric and Gravity Measurements for Groundwater Exploration and Detection of Structural Elements at Romana Area, Northwest of Sinai, Egypt", in *Proceedings of the 6th Conf. Geology of Sinai for Development, Ismailia*, 2001, pp. 109–120.

[5] F. A. M. Monteiro Santos, S. A. Sultan, R. Patrıcia, and A. L. El Sorady, "Joint Inversion of Gravity and Geoelectrical Data for Groundwater and Structural Investigation: Application to the Northwestern Part of Sinai, Egypt", *Geophys. J. Int*., **165**(2006), pp. 705–718.

[6] UNESCO Cairo Office, *Geologic Map of Sinai, Egypt, Scale 1:500,000, Project for the Capacity Building of the Egyptian Geological survey and Mining Authority and the National Authority for Remote Sensing and Space Science in Cooperation with UNDP and UNESCO*. Geological Survey of Egypt, 2004.

[7] O. Koefoed, "A Generalized Cagniard Graph for Interpretation of Geoelectric Sounding Data", *Geophysical Prospecting*, **8**(**3**)(1960), pp.459–469.

[8] *Geosoftw Program (Oasis Montaj)*. Geosoft Mapping and Application System, Inc, Suit 500, Richmond St. West Toronto, ON Canada N5SIV6, 1998.

[9] V. Baranov, "A New Method for Interpretation of Aeromagnetic Maps: Pseudo- Gravimetric Anomalies", *Geophysics*, **22**(1957), pp. 359–383.

[10] V. Baranov, and H. Naudy, "Numerical Calculation of the Formula of Reduction to the Magnetic Pole", *Geophysics*, **29**(1964), pp. 67–79.

[11] B. K. Bhattacharyya, "Two Dimensional Harmonic Analysis as a Tool for Magnetic Interpretation", *Geophysics*, **30**(**5**)(1965), pp. 829 – 857.

[12] B. K. Bhattacharyya, "Some General Properties of Potential Field in Space and Frequency Domains", *Review Geoexploration*, **5**(1967), pp. 127–143.

[13] V. Baranov, "Potential Fields and Their Transformation in Applied Geophysics", *Geoexploration Monographs, Series* 1-6. Berlin – Stuttgart: Gebrüder, Borntraeger, 1975

[14] D.T.T. Thompson, "Euler, a New Technique for Making Computer Assisted Depth Estimates from Magnetic Data", Geophysics, **47**(1982) pp. 31–37.

[15] M. B. Dobrin, *Introduction to Geophysical Prospecting*. New York: McGraw-Hill, 1988, 867 pp.